High-pressure oxidation of propane

Hashemi, Hamid; Christensen, Jakob M.; Harding, Lawrence B.; Klippenstein, Stephen J.; Glarborg, Peter

Published in:
Proceedings of the Combustion Institute

Link to article, DOI:
10.1016/j.proci.2018.07.009

Publication date:
2019

Document Version
Peer reviewed version

High-Pressure Oxidation of Propane

Hamid Hashemi*[a], Jakob M. Christensen[a], Lawrence B. Harding[b], Stephen J. Klippenstein[b], Peter Glarborg[a]

[a] *DTU Chemical Engineering, Technical University of Denmark, DK-2800 Lyngby, Denmark*
[b] *Chemical Sciences and Engineering Division, Argonne National Laboratory, Argonne, IL 60439, USA*

Abstract

The oxidation properties of propane have been investigated by conducting experiments in a laminar flow reactor at a pressure of 100 bar and temperatures of 500–900 K. The onset temperature for reaction increased from 625 K under oxidizing conditions to 725 K under reducing conditions. A chemical kinetic model for high pressure propane oxidation was established, with particular emphasis on the peroxide chemistry. The rate constant for the important abstraction reaction $C_3H_8 + HO_2$ was calculated theoretically. Modeling predictions were in satisfactory agreement with the present data as well as shock tube data (6–61 bar) and flame speeds (1–5 bar) from literature.

Keywords:

Propane, Combustion, High pressure, Reaction kinetics, LPG

1. Introduction

The oxidation properties of propane, a major component of liquified propane gas (LPG) and a minor but sensitive component in natural gas have attracted research and industrial interests. Under certain conditions, propane oxidation is inhibited by increasing temperature. This behaviour, more frequent for heavier alkanes, is called Negative Temperature Coefficient (NTC). The NTC behaviour increases the complexity of chemical kinetic modeling. The temperature range at which NTC is observed for propane depends on pressure and mixture composition, but it generally occurs at temperatures below 1000 K [1–4].

*Corresponding author: hah@kt.dtu.dk, URL: http://www.kt.dtu.dk

Flow reactors are suitable devices to investigate combustion chemistry at intermediate temperatures, but they have rarely been used to study the oxidation properties of propane. Notably, Cathonnet et al. [5] and Cord et al. [6] measured propane oxidation in a jet-stirred reactor at pressures below 6 bar and Koert et al. [7] measured species evolution in a turbulent flow reactor at pressures of 10–15 atm.

The ignition delay time of propane has been investigated more extensively, using mostly shock tubes [1, 2, 8–14] and Rapid Compression Machines [3, 4]. Several of these studies were conducted at elevated pressure, i.e., up to 60 bar in shock tubes [1, 2, 8, 12, 13] and 37 bar in RCM [3, 4]. Data have also been reported from a batch reactor at up to 15 bar [15] and from a test engine [16]. Despite the extensive measurements of ignition properties, the investigated pressures are thus far below those found in engines.

Several detailed chemical kinetic models have been developed and evaluated for propane oxidation, e.g., [17–21]. The models developed by Jachimowski [17], Frenklach and Bornside [18], Dagaut et al. [19], and Koert et al. [20] were evaluated at a maximum pressure of 15 atm. Qin et al. [21] optimized a detailed chemical kinetic model against ignition delays at P<5 atm and flame data at atmospheric pressure. This optimized model has been widely adopted in subsequent flame studies (e.g. [22–25]). More recently, Petersen et al. [26] developed a mechanism for mixtures of propane and methane. Due to the lack of experimental data at high pressures, the developed mechanisms were validated at pressures below those found in engines.

To extend the available data toward conditions relevant to engines and gas turbines, this paper reports the results of propane oxidation experiments in a laminar flow reactor at a pressure of 100 bar and temperatures of 500–900 K under a wide range of stoichiometries. A chemical kinetic model for propane oxidation at increased pressure is established by carefully reviewing available thermo-kinetic data in literature. For the key step between propane and the HO_2 radical, the rate constant was calculated from theory.

2. Experimental

2.1. The laminar flow reactor

The experimental setup was a laboratory-scale high-pressure laminar flow reactor designed to approximate plug flow. The setup is described in detail elsewhere [27] and only a brief description is provided here. The system was used here for investigation of propane oxidation at 100 bar pressure and temperatures up to 900 K. The reactant gases were premixed before entering the reactor. The reactions took place in a tubular quartz reactor with an inner diameter of 8 mm and a total length of 154.5 cm.

The reactor was heated by three digitally controlled heating elements. The measured temperature profile of the reactor can be found in Supplementary material. The profile showed an isothermal reaction zone (±6 K under inert conditions) of 38–40 cm. The residence time in the isothermal zone was 8.3–14 s with the current flow rate of 3.93 liter/min (STP) and temperatures in the range of 500–900 K. The maximum adiabatic temperature-rise due to heat of reaction was calculated to be 8 K. All gases used in the present experiments were high purity gases or mixtures with certified concentrations (±2% uncertainty). The product analysis was conducted by an on-line *6890N Agilent Gas Chromatograph* (GC-TCD/FID) equipped with three columns (Porapak N, Molsieve 13X, and PoraPLOT Q). For most species, the relative measuring uncertainty of the GC was in the range of ±10%.

3. Numerical

A chemical kinetic model for propane oxidation at increased pressure was established. The C_3 subset, which is briefly discussed below, was added to the reaction mechanism developed earlier for the oxidation of $H_2/C_1/C_2$ and oxygenated components [28–33]. The reaction of C_3H_8 with HO_2, which is a key step at high pressure, was studied theoretically, as described below.

3.1. Theory for C_3H_8 + HO_2

The rovibrational properties of C_3H_8, HO_2, and the two H atom abstraction transition states to produce *i*- and *n*-propyl radicals were determined at the CASPT2/cc-pVTZ level.

For the transition states, a 5-electron 5-orbital (5e,5o) active space was employed, with the orbitals correlating with the HO_2 radical orbital, and one σ,σ^* pair for both of the central and terminal CH bonds. The corresponding (4e,4o) σ,σ^* active space was employed for C_3H_8 and a (1e,1o) active space was employed for HO_2.

Higher level estimates of the energies at these stationary points were obtained from CCSD(T) calculations with the cc-pVTZ and cc-pVQZ basis sets extrapolated to the complete basis set limit. The zero-point corrected CCSD(T)/CBS energies were 19.3 and 16.6 kcal/mol (relative to reactants) for the transition states to form *i*- and *n*-C_3H_7. The rate constant was predicted with conventional transition state theory employing rigid rotor harmonic oscillator assumptions for all but the torsional modes, which were treated as 1-dimensional hindered rotors. Eckart tunneling corrections were included.

The calculated rate constants for $C_3H_8 + HO_2 \rightarrow$ *n*-$C_3H_7 + H_2O_2$ (R4a) and $C_3H_8 + HO_2 \rightarrow$ *i*-$C_3H_7 + H_2O_2$ (R4b) are $k_{4a} = 0.27\ (T/K)^{4.125}\ \exp(-7638/T)\ cm^3\ mol^{-1}\ s^{-1}$ and $k_{4b} = 6.32\ (T/K)^{3.670}\ \exp(-6752/T)\ cm^3\ mol^{-1}\ s^{-1}$, respectively. From prior experience with calculations performed at similar levels of theory we estimate the 2 sigma uncertainty in the rate predictions to be a factor of 3. Only indirect measurements by Walker and coworkers [34–36] have been reported for the reaction. As illustrated in Figs. 1 and 2, the calculated values are in good agreement with the most recent data of Handford-Styring and Walker [36]. Earlier CCSD(T)/cc-pVTZ//B3LYP based TST calculations of Simmie and coworkers [37], which are renormalized to estimates of the CCSD(T)/CBS limit for abstraction from CH_4, are very similar to the present ones. In contrast, the CBS-QB3 based predictions of Deutschmann and coworkers [38] appear to substantially overestimate the abstraction rates.

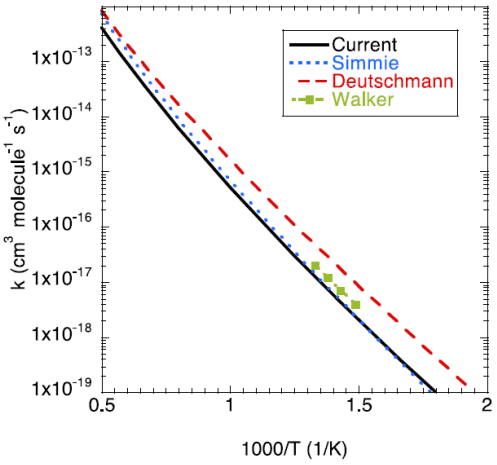

Figure 1: Plot of the rate constant for $C_3H_8 + HO_2 \rightarrow CH_3CH_2CH_2 + H_2O$ (R4a). The current value is compared with experimental data from Handford-Styring and Walker [36] and predictions of Simmie and coworkers [37] and Deutschmann and coworkers [38].

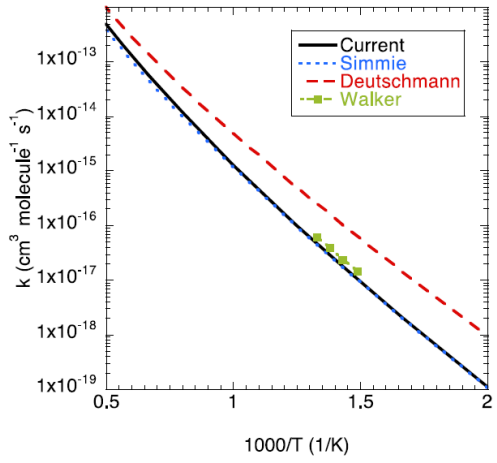

Figure 2: Plot of the rate constant for $C_3H_8 + HO_2 \rightarrow CH_3CHCH_3 + H_2O$ (R4b). The current value is compared with experimental data from Handford-Styring and Walker [36] and predictions of Simmie and coworkers [37] and Deutschmann and coworkers [38].

3.2. The propane subset of the kinetic model

The propane subset added in the present work includes reactions of C_3H_8 and the derived radicals. For interpreting reaction numbers, readers are suggested to consult the reaction list in the Supplementary material. Selected reactions are shown in Table 1. Hydrogen abstraction from propane results in the two isomers, normalpropyl (n-C_3H_7) and isopropyl (i-C_3H_7), adding to the complexity of the combustion chemistry of this fuel. Rate constants for propane consumption reactions were mostly drawn from shock tube and theoretical work of Sivaramakrishnan and coworkers, including those for thermal dissociation (C_3H_8 (+M) = C_2H_5 + CH_3 (+M) (R1)) [39] and for hydrogen-abstraction reactions with H (R2) [40] and OH (R3) [41].

The results of Sivaramakrishnan et al. [41] for $C_3H_8 + OH$ (R3) (obtained at 797–1259 K and extrapolated from theory to 250–2000 K) have been confirmed by more recent measurements by Morin et al. [42] (230–900 K) and by Badra et al. [43] (895–1294 K). The theoretical work indicates a slightly lower branching fraction to n-C_3H_7 than indicated by earlier experiments by Droege and Tully [44].

The reaction of propane with the hydroperoxyl radical (R4), studied in the present work, would be expected to be a rate limiting step for low temperature ignition of propane, similar to observations for lighter alkanes (methane and ethane) [29, 31]. Also H-abstraction by alkylperoxyl radicals has been shown to be important in the oxidation of methane and ethane at high pressure [29, 31]. For reaction with CH_3OO (R7) and CH_3CH_2OO (R8), we rely on the calculated rate constants of Carstensen et al. [38], while the values for abstraction by the C_3H_7OO isomers (R9, R10) were estimated by analogy to the $C_3H_8 + CH_3CH_2OO$ reaction.

The propyl radicals n-C_3H_7 and i-C_3H_7 may decompose at elevated temperature or react with O_2. For the decomposition steps (R11, R12), we adopted the rate constants from the theoretical study by Miller and Klippenstein [45]. Oxygen addition to propyl to form isomers of propylperoxyl radicals (C_3H_7OO (R13, R14)) is important at intermediate temperature; these reactions were studied theoretically by Goldsmith et al. [46] and implemented here.

The propylperoxyl radicals can isomerize (R15, R20) to the propylhydroperoxyl radical C_3H_6OOH, which may undergo further internal H-abstraction (R16) before dissociating to $C_3H_6 + HO_2$ (R17–R19, R21, R22). A second oxygen addition to propylhydroperoxyl radicals to form isomers of OOC_3H_6OOH is expected to be a critical step in low-temperature oxidation of alkanes. The OOC_3H_6OOH formed may decompose or isomerize to $HOOC_3H_5OOH$. Data for these reactions, as well as those of C_3H_6OOH, were also drawn from Goldsmith et al. [46].

Table 1: Selected reactions from the C_3 subset of the present model. The rate constants are in the form of $k = AT^n \exp(-E/(RT))$. Units are mol, cm, K, s, and cal.

	Reaction	A	n	E	Note/Ref.
R3a	$C_3H_8 + OH \rightleftarrows nC_3H_7 + H_2O$	5.2E03	2.936	-419	[41]
R3b	$C_3H_8 + OH \rightleftarrows iC_3H_7 + H_2O$	1.8E05	2.437	-536	[41]
R4a	$C_3H_8 + HO_2 \rightleftarrows nC_3H_7 + H_2O_2$	2.7E-01	4.125	15176	p.w.
R4b	$C_3H_8 + HO_2 \rightleftarrows iC_3H_7 + H_2O_2$	6.3E00	3.670	13416	p.w.
R7a	$C_3H_8 + CH_3OO \rightleftarrows nC_3H_7 + CH_3OOH$	6.7E00	3.720	16900	[38]
R7b	$C_3H_8 + CH_3OO \rightleftarrows iC_3H_7 + CH_3OOH$	8.1E01	3.370	13800	[38]
R15	$nC_3H_7OO \rightleftarrows CH_2CH_2CH_2OOH$	3.4E00	3.230	19209	[a] [46]
	Duplicate rate constant	4.1E26	-0.037	99401	
R18	$nC_3H_7OO \rightleftarrows C_3H_6 + HO_2$	2.3E32	-6.220	37948	[a] [46]
R32	$HOOCCCOO^* \rightleftarrows OCCCOOH + OH$	1.7E05	1.480	16238	[a] [46]

[a] At 100 atm pressure, for other pressures see the mechanism file in Supplementary material.

4. Results and discussion

4.1. Oxidation in the flow reactor

Figure 3 shows the results of propane oxidation under reducing conditions. Reaction started at 700–725 K and the major products were CO, C_3H_6, CH_4, and C_2H_4. The maximum carbon deficiency from the experiments was around 7%. Using the current analysing equipment, it was not possible to measure C_2H_3CHO and CH_2O. Adding their concentrations from simulations, carbon balanced within ±5%. The model reproduces the onset of oxidation, as well as the concentrations of most intermediates satisfactorily. However, there are discrepancies between model predictions and experimental data for CH_3CHO and

C_2H_5CHO. It was found that using a full temperature profile for modeling in CHEMKIN [47] improved the accuracy of the simulation. Therefore, a plug flow reactor with a fixed temperature profile and constrained pressure was used for all simulations. The profiles used in modeling can be found as Supplementary material.

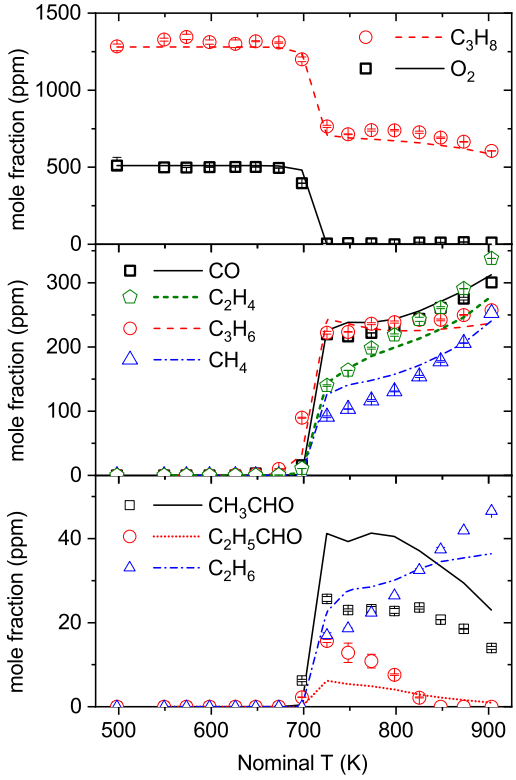

Figure 3: Results of experiments under reducing conditions (1285 ppm C_3H_8 and 511 ppm O_2 in N_2, Φ=12.5) at 100 bar pressure. Symbols mark the experimental results and lines denote the predictions of the present model.

Figure 4 shows the results of propane oxidation for a stoichiometric mixture. The fuel conversion started around 725 K, where a small fraction of propane disappeared and trace amounts of C_3H_6 and C_2H_4 were detected. At T>750 K, propane was oxidized almost completely. The major products of the oxidation were CO and CO_2 and the concentration of propene and ethene decreased sharply at temperatures higher than 775 K. The carbon balance showed a maximum deficiency of around 19%. Adding C_2H_3CHO and CH_2O from simulation, carbon balanced within $\pm$11%.

The model captured the onset temperature of ignition accurately. However, CO oxidation

to CO_2 at high temperatures was not precisely captured by the model.

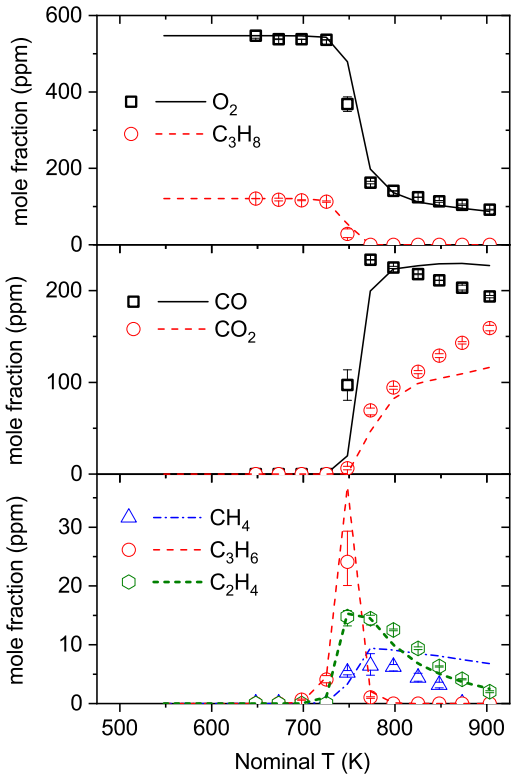

Figure 4: Results of experiments under stoichiometric conditions (547 ppm O_2 and 121 ppm C_3H_8 in N_2, Φ=1.1) at 100 bar pressure. Symbols mark the experimental results and lines denote the predictions of the present model.

The fuel-lean experiments shown in Fig. 5 revealed a sharp onset of reaction for propane concentration at 625 K, and propane was completely consumed at T>725 K. The major detected products were CO and CO_2. The carbon balance showed a maximum deviation of 18% (at 675 K). The model captured the onset of oxidation accurately, but underpredicted the reactivity and thereby the fuel conversion at higher temperatures. Propene, a minor by-product, was slightly overpredicted by the model.

The experimental results and the modeling predictions do not support occurrence of NTC behaviour in propane oxidation under the conditions investigated here. Herzler et al. [1] and Cadman et al. [2] measured ignition delays of propane/air in shock tubes (ϕ = 0.5, P=10–40 bar) and reported a decrease in the activation energy of ignition delays at T<1050 K, but NTC behaviour was not observed even at temperatures as low as 875 K. In a more recent

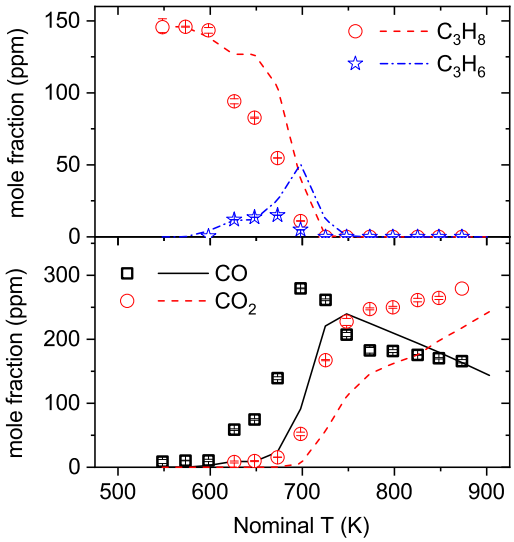

Figure 5: Results of experiments under oxidizing conditions (3.405% O_2 and 146 ppm C_3H_8 in N_2, Φ=0.02) at 100 bar pressure. Symbols mark the experimental results and lines denote the predictions of the present model.

study, Lam et al. [13] found no evidence of NTC behaviour for propane/oxygen/argon at 980–1400 K and 6–60 atm ($\phi = 0.5$). On the other hand, NTC behaviour for propane/air ignition delays measured in an RCM has been reported by Gallagher et al. [3] at temperatures of 750–825 K ($\phi = 0.5$, P=27–37 atm) and by Dames et al. [4] at 760–800 K (ϕ =0.5/1.0, P $\simeq$30 atm). The RCM experiments cover partially the same temperature range as our flow reactor experiments. The difference in NTC behaviour is possibly due to the higher dilution of reactants in the present experiments. To test this hypothesis, we conducted flow reactor simulations at higher initial concentrations of propane. The results (shown in Supplementary material) indicate that at higher reactant concentrations a plateau, which represents NTC, occurs between 600 and 650 K. Also, simulations of ignition delay times show that the NTC temperature interval becomes broader when the initial concentrations of propane and oxygen are increased (see SM).

A reaction pathway analysis for propane oxidation (Fig. 6) shows that at 750 K, propane is mainly oxidized by reaction with OH and HO_2 (R3, R4). If the H-abstraction steps yield the i-C_3H_7 radical, it will add to molecular oxygen to give i-C_3H_7OO, which eventually decomposes to propene. If n-C_3H_7 is formed, then decomposition to ethene competes with

the addition of molecular oxygen to form the peroxide.

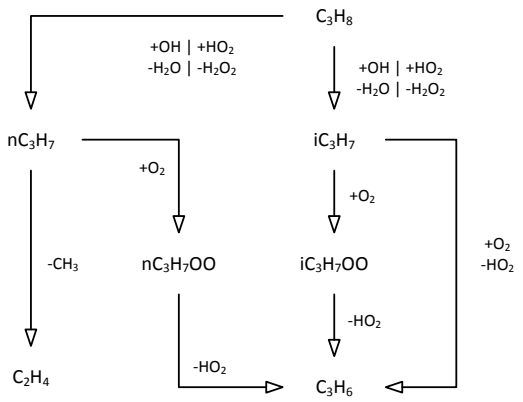

Figure 6: Reaction pathways for propane conversion to alkenes under stoichiometric and oxidizing conditions (750 K, 100 bar). The detailed pathway can be found in Supplementary material.

According to the results of sensitivity analyses (Fig. 7), propane oxidation is largely controlled by H-abstraction from propane by OH and HO_2. For abstraction by OH, the branch to *n*-C_3H_7 (R3a) promotes the oxidation for reducing and stoichiometric conditions while the channel to *i*-C_3H_7 (R3b) inhibits the oxidation. For abstraction by HO_2 (R4), even the channel to *i*-C_3H_7 (R4b) promotes oxidation due to differences in reactivity between the HO_2 and C_3H_7OO peroxide radicals. In addition to these steps, H-abstraction from propane by CH_3OO (R7, $C_3H_8 + CH_3OO = iC_3H_7 + CH_3OOH$) is important for reducing and stoichiometric conditions.

4.2. Comparison with literature data

4.2.1. Ignition delay time

Figure 8 compares reported ignition delay times for propane at pressures of 10–60 bar with those predicted by the model. The model agrees well with data measured in a shock tube under near-constant-volume test conditions [13], but it overestimates ignition delays at T<1100 K for the conditions of Herzler et al. [1] and Cadman et al. [2]. Lam et al. [13] found it important to include effects of pressure and temperature variations prior to ignition in interpreting and simulating data from conventional shock tubes for long ignition delays. The discrepancies between the model predictions and the experiments in [1, 2] may

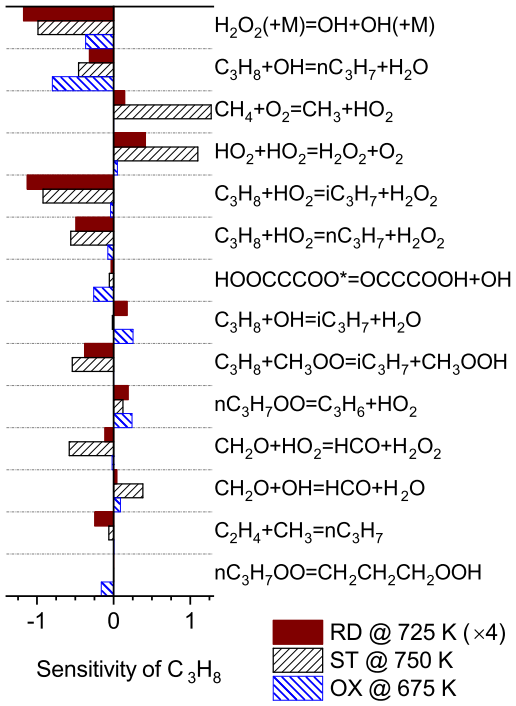

Figure 7: Sensitivity of C_3H_8 prediction under flow-reactor conditions (RD: reducing, ST: stoichiometric, OX: oxidizing conditions) at 100 bar. Only the isothermal part of the reactor was considered in the simulations. The residence time was adjusted to achieve 20% conversion of C_3H_8. For reducing conditions, coefficients are enlarged 4 times for better representation. $HOOCCCOO^*$ and OCCCOOH are abbreviations for $HOOCH_2CH_2CH_2OO^*$ and $OCHCH_2CH_2OOH$, respectively.

partly be attributed to the lack of such treatment in our simulations; the pressure histories of individual ignition delay measurements were not available.

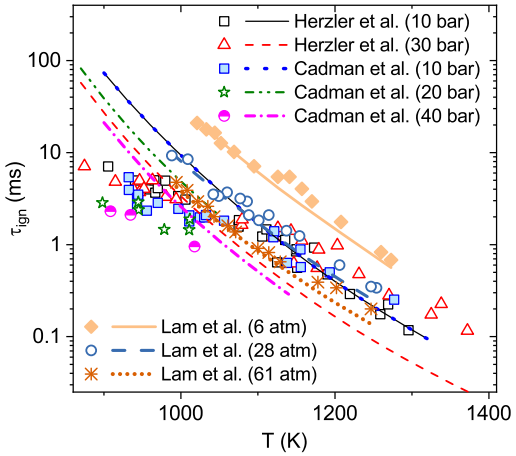

Figure 8: Ignition delay times of propane/oxygen/inert mixtures. Symbols mark experimental results from Herzler et al. [1] and Cadman et al. [2] (2.1% C_3H_8 + 20.6% O_2 in N_2, Φ=0.5) and Lam et al. [13] (0.8% C_3H_8 + 8% O_2 in Ar, Φ=0.5). Lines denotes the predictions of the present model. Data from [13] were simulated at average pressure and only those points that were within ± 12 % of the average pressure are shown here. A higher resolution of this plot can be found in Supplementary material.

A sensitivity analysis is performed for ignition delay times of propane at 10–30 bar and 900–1200 K. The results can be found in the Supplementary material. The H-abstraction by HO_2 from propane is sensitive in determining ignition delays. At the lower pressure of 10 bar, the reaction of $CH_3 + HO_2 = CH_4 + O_2$ inhibits ignition. The sensitivity coefficients for $C_3H_8 + OH = n\text{-}C_3H_7 + H_2O$ (R3a) and $n\text{-}C_3H_7 = C_2H_4 + CH_3$ (R11b) are noteworthy, as both steps accelerate ignition at 900 K but inhibit reaction at 1100 K (30 bar).

4.2.2. Flame speed

Figure 9 compares flame speeds of propane/air predicted by the current model with those measured in literature [48–56]. The flame speed decreases at elevated pressures. The model predictions are within the uncertainty range of the data.

To identify reactions sensitive for predicting the flame speed, the sensitivity of the mass flow rate is calculated using the built-in functions of Chemkin [47]. The results can be found in the Supplementary material. Most of the sensitive reactions belong to H_2, C_1 and C_2 subsets, which are adopted from our earlier work [28–31]. The model predicts the flame

speeds of H_2, CH_4, C_2H_2, and C_2H_4 well [28–31], but overpredicts the burning velocities of ethane [31] and ethanol [33].

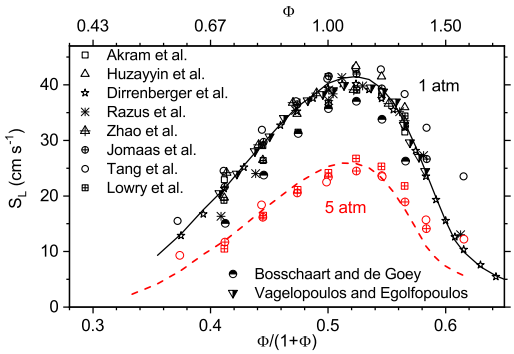

Figure 9: Laminar burning velocity of propane/air mixture at 1 and 5 atm and initial temperature of 300 K. Symbols mark experimental results from Vagelopoulos and Egolfopoulos [48], Zhao et al. [49], Bosschaart and De Goey [50], Jomaas et al. [51], Huzayyin et al. [52], Tang et al. [53], Lowry et al. [54], Dirrenberger et al. [55], Razus et al. [56], and Akram et al. [24]. Lines denote the model prediction at specified pressures.

5. Conclusion

Propane oxidation at high pressure (100 bar) and intermediate temperature (500–900 K) has been investigated in a flow reactor as a function of stoichiometry. These data extend the propane oxidation benchmark at high pressures and intermediate temperatures. The onset of fuel oxidation was found to be 625–725 K, increasing with fuel-air equivalence ratio. The rate constant for the reaction $C_3H_8 + HO_2$ was calculated theoretically. A detailed chemical kinetic model for propane oxidation at high pressure was developed and evaluated against the present data as well as results from literature. The model agreed well with the flow reactor data, even though it slightly underpredicted the fuel conversion under fuel-lean conditions. Sensitivity analyses revealed the importance of H-abstraction reactions by HO_2, OH, and CH_3OO in controlling propane oxidation at 750 K. Modeling predictions were also in satisfactory agreement with reported ignition delay times and flame speeds.

Acknowledgments

Funding from *MAN Diesel & Turbo* and *Technical University of Denmark* is gratefully acknowledged. This project has received funding from the *European Union's Horizon 2020*

research and innovation program under grant agreement no. 634135 HERCULES-2. Part of this material is based on work at Argonne supported by the U.S. Department of Energy, Office of Basic Energy Sciences, Division of Chemical Sciences, Geosciences, and Biosciences, under Contract No. DE-AC02-06CH11357 as part of the Argonne-Sandia Consortium on High-Pressure Combustion Chemistry (ANL FWP # 59044).

References

[1] J. Herzler, L. Jerig, P. Roth, Combust. Sci. Technol. 176 (2004) 1627–1637.

[2] P. Cadman, G. O. Thomas, P. Butler, Phys. Chem. Chem. Phys. 2 (2000) 5411–5419.

[3] S. M. Gallagher, H. J. Curran, W. K. Metcalfe, D. Healy, J. M. Simmie, G. Bourque, Combust. Flame 153 (2008) 316–333.

[4] E. E. Dames, A. S. Rosen, B. W. Weber, C. W. Gao, C.-J. Sung, W. H. Green, Combust. Flame 168 (2016) 310–330.

[5] M. Cathonnet, J. C. Boettner, H. James, Symp. Combust. 18 (1981) 903–913.

[6] M. Cord, B. Husson, J. C. Lizardo Huerta, O. Herbinet, P.-A. Glaude, R. Fournet, B. Sirjean, F. Battin-Leclerc, M. Ruiz-Lopez, Z. Wang, M. Xie, Z. Cheng, F. Qi, J. Phys. Chem. A 116 (2012) 12214–12228.

[7] D. N. Koert, D. L. Miller, N. P. Cernansky, Combust. Flame 96 (1994) 34–49.

[8] A. Burcat, K. Scheller, A. Lifshitz, Combust. Flame 16 (1971) 29–33.

[9] C. J. Brown, G. O. Thomas, Combust. Flame 117 (1999) 861–870.

[10] D. F. Davidson, J. T. Herbon, D. C. Horning, R. K. Hanson, Int. J. Chem. Kinet. 33 (2001) 775–783.

[11] D. Horning, D. Davidson, R. Hanson, J. Propul. Power 18 (2002) 363–371.

[12] O. Penyazkov, K. Ragotner, A. Dean, B. Varatharajan, Proc. Combust. Inst. 30 (2005) 1941–1947.

[13] K.-Y. Lam, Z. Hong, D. Davidson, R. Hanson, Proc. Combust. Inst. 33 (2011) 251–258.

[14] G. Agafonov, A. Tereza, Russ. J. Phys. Chem. B 9 (2015) 92–103.

[15] F. Norman, F. V. den Schoor, F. Verplaetsen, J. Hazard. Mater. 137 (2006) 666–671.

[16] K. J. Morganti, M. J. Brear, G. da Silva, Y. Yang, F. L. Dryer, Proc. Combust. Inst. 35 (2015) 2933–2940.

[17] C. J. Jachimowski, Combust. Flame 55 (1984) 213–224.

[18] M. Frenklach, D. E. Bornside, Combust. Flame 56 (1984) 1–27.

[19] P. Dagaut, M. Cathonnet, J.-C. Boettner, Int. J. Chem. Kinet. 24 (1992) 813–837.

[20] D. N. Koert, W. J. Pit, J. W. Boelli, N. P. Cernansky, Symp. (Int.) Combust., [Proc.] 26 (1996) 633–640.

[21] Z. Qin, V. V. Lissianski, H. Yang, W. C. Gardiner, S. G. Davis, H. Wang, Proc. Combust. Inst. 28 (2000) 1663–1669.

[22] Z. Zhao, A. Kazakov, J. Li, F. L. Dryer, Combust. Sci. Technol. 176 (2004) 1705–1723.

[23] Z. Cheng, R. W. Pitz, J. A. Wehrmeyer, Combust. Flame 145 (2006) 647–662.

[24] M. Akram, V. R. Kishore, S. Kumar, Energy Fuels 26 (2012) 5509–5518.

[25] C. A. Cardona, A. A. Amell, Int. J. Hydrogen Energy 38 (2013) 7994–8001.

[26] E. L. Petersen, D. M. Kalitan, S. Simmons, G. Bourque, H. J. Curran, J. M. Simmie, Proc. Combust. Inst. 31 (2007) 447–454.

[27] C. L. Rasmussen, J. Hansen, P. Marshall, P. Glarborg, Int. J. Chem. Kinet. 40 (2008) 454–480.

[28] H. Hashemi, J. M. Christensen, S. Gersen, P. Glarborg, Proc. Combust. Inst. 35 (2015) 553–560.

[29] H. Hashemi, J. M. Christensen, S. Gersen, H. Levinsky, S. J. Klippenstein, P. Glarborg, Combust. Flame 172 (2016) 349–364.

[30] J. Lopez, C. Rasmussen, H. Hashemi, M. Alzueta, Y. Gao, P. Marshall, C. Goldsmith, P. Glarborg, Int. J. Chem. Kinet. 48 (2016) 724–738.

[31] H. Hashemi, J. G. Jacobsen, C. T. Rasmussen, J. M. Christensen, P. Glarborg, S. Gersen, M. van Essen, H. B. Levinsky, S. J. Klippenstein, Combust. Flame 182 (2017) 150–166.

[32] V. Aranda, J. M. Christensen, M. U. Alzueta, P. Glarborg, S. Gersen, Y. Gao, P. Marshall, Int. J. Chem. Kinet. 45 (2013) 283–294.

[33] H. Hashemi, J. M. Christensen, P. Glarborg, Fuel 218 (2018) 247–257.

[34] R. Baldwin, D. Langford, M. Matchan, R. Walker, D. Yorke, Symp. (Int.) Combust. 13 (1971) 251.

[35] R. Baldwin, A. Fuller, D. Longthorn, R. Walker, in: F. J. Weinberg (Ed.), Combust. Inst. European Symp., Academic Press, London, 1973.

[36] S. Handford-Styring, R. Walker, Phys Chem. Chem. Phys. 4 (2002) 620–627.

[37] J. Aguilera-Iparraguirre, H. J. Curran, W. Klopper, J. M. Simmie, J. Phys. Chem. A 112 (2008) 7047–7054.

[38] H.-H. Carstensen, A. M. Dean, O. Deutschmann, Proc. Combust. Inst. 31 (2007) 149–157.

[39] R. Sivaramakrishnan, M.-C. Su, J. V. Michael, S. J. Klippenstein, L. B. Harding, B. Ruscic, J. Phys. Chem. A 115 (2011) 3366–3379.

[40] R. Sivaramakrishnan, J. V. Michael, B. Ruscic, International Journal of Chemical Kinetics 44 (2012) 194–205.

[41] R. Sivaramakrishnan, N. Srinivasan, M.-C. Su, J. V. Michael, Proc. Combust. Inst. 32 (2009) 107–114.

[42] J. Morin, M. N. Romanias, Y. Bedjanian, Int. J. Chem. Kinet. 47 (2015) 629–637.

[43] J. Badra, E. F. Nasir, A. Farooq, J. Phys. Chem. A 118 (2014) 4652–4660.

[44] A. T. Droege, F. P. Tully, The Journal of Physical Chemistry 90 (1986) 1949–1954.

[45] J. A. Miller, S. J. Klippenstein, J. Phys. Chem. A 117 (2013) 2718–2727.

[46] C. F. Goldsmith, W. H. Green, S. J. Klippenstein, J. Phys. Chem. A 116 (2012) 3325–3346.

[47] Ansys 17.2 Chemkin-Pro, 2017.

[48] C. M. Vagelopoulos, F. N. Egolfopoulos, Symp. (Int.) Combust., [Proc.] 27 (1998) 513–519.

[49] Z. Zhao, A. Kazakov, J. Li, F. L. Dryer, Combustion science and technology 176 (2004) 1705–1723.

[50] K. Bosschaart, L. De Goey, Combust. Flame 136 (2004) 261–269.

[51] G. Jomaas, X. L. Zheng, D. L. Zhu, C. K. Law, Proc. Combust. Inst. 30 (2005) 193–200.

[52] A. Huzayyin, H. Moneib, M. Shehatta, A. Attia, Fuel 87 (2008) 39–57.

[53] C. Tang, J. Zheng, Z. Huang, J. Wang, Energy Convers. Manag. 51 (2010) 288–295.

[54] W. Lowry, J. de Vries, M. Krejci, E. Petersen, Z. Serinyel, W. Metcalfe, H. Curran, G. Bourque, J. Eng. Gas Turbines Power 133 (2011) 91501.

[55] P. Dirrenberger, H. Le Gall, R. Bounaceur, O. Herbinet, P.-A. Glaude, A. Konnov, F. Battin-Leclerc, Energy Fuels 25 (2011) 3875–3884.

[56] D. Razus, V. Brinzea, M. Mitu, C. Movileanu, D. Oancea, Energy & Fuels 26 (2012) 901–909.